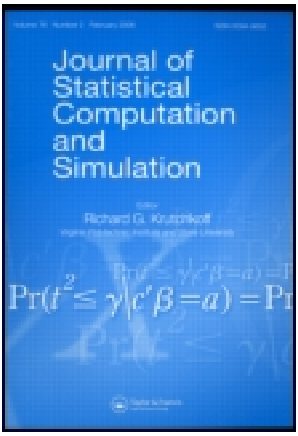

Journal of Statistical Computation and Simulation
Publication details, including instructions for authors and subscription information:
http://www.tandfonline.com/loi/gscs20

A bootstrap control chart for inverse Gaussian percentiles

Y. L. Lio [a] & Chanseok Park [b]
[a] Department of Mathematical Sciences, University of South Dakota, Vermilion, SD, USA
[b] Department of Mathematical Sciences, Clemson University, Clemson, SC, USA
Published online: 13 Feb 2009.

Journal of Statistical Computation and Simulation
Vol. 80, No. 3, March 2010, 287–299

A bootstrap control chart for inverse Gaussian percentiles

Y.L. Lio[a]* and Chanseok Park[b]

[a]*Department of Mathematical Sciences, University of South Dakota, Vermilion, SD, USA;* [b]*Department of Mathematical Sciences, Clemson University, Clemson, SC, USA*

(*Received 10 July 2008; final version received 16 November 2008*)

The conventional Shewhart-type control chart is developed essentially on the central limit theorem. Thus, the Shewhart-type control chart performs particularly well when the observed process data come from a near-normal distribution. On the other hand, when the underlying distribution is unknown or non-normal, the sampling distribution of a parameter estimator may not be available theoretically. In this case, the Shewhart-type charts are not available. Thus, in this paper, we propose a parametric bootstrap control chart for monitoring percentiles when process measurements have an inverse Gaussian distribution. Through extensive Monte Carlo simulations, we investigate the behaviour and performance of the proposed bootstrap percentile charts. The average run lengths of the proposed percentage charts are investigated.

Keywords: average run length (ARL); inverse Gaussian (Wald) distribution; control charts; false alarm rate; parametric bootstrap; percentile; Shewhart chart

AMS (2000) Subject Classification: Primary: 62F40; Secondary: 62P30

1. Introduction

The inverse Gaussian distribution, also known as the Wald distribution, has been recognized as a versatile lifetime model with sound physical interpretation and has been used as a failure time model for a variety of applications, for example in fatigue by Bhattacharyya and Fries [1] and in general stochastic wear-out by Desmond [2] and Goh *et al.* [3]. More applications of the inverse Gaussian distribution are detailed by Chhikara and Folks [4]. Since the sampling distributions for the estimators of inverse Gaussian location and scale parameters were easily derived, control charts for detecting the shifts of centrality and of variability for the inverse Gaussian distribution have been developed by several papers such as Edgeman [5–7], Hawkins and Olwell [8] and Sim [9].

In industrial applications, specific limits of the lifetime for a device are usually required for engineering design considerations. Therefore, it is imperative that one could provide a control chart for inverse Gaussian percentiles. However, the sampling distribution of the inverse Gaussian percentile estimator is mathematically intractable. Moreover, the relationship between inverse Gaussian percentiles and inverse Gaussian parameters are not explicitly available. Under a small sample size, the sampling distributions for estimators of the inverse Gaussian location and of scale

*Corresponding author. Email: Yuhlong.Lio@usd.edu

ISSN 0094-9655 print/ISSN 1563-5163 online

DOI: 10.1080/00949650802627402
http://www.informaworld.com

parameters cannot be used to construct the quality control charts of inverse Gaussian percentiles. In this case, computational methods, such as parametric or nonparametric bootstrap methods, can be used to set control limits for appropriate control charts of inverse Gaussian percentiles; see [10–12] for a basic discussion of bootstrap techniques. An advantage of the bootstrap methods is that they are not restricted by assumptions on the distribution of the process measurements. The computation time of the method is perhaps a perceived disadvantage, but actually is not, given the current computing power available and considering the possibility of using an inappropriate control chart. Also, with the advent of modern powerful and accessible computers, simulation-based estimation such as bootstrapping is more easily obtained than before. The bootstrap method uses only the sample data to estimate the sampling distribution of the interesting parameter estimator and then to determine appropriate control limits. Only the usual assumptions (for Phase II of the statistical process control paradigm), that the process is stable and subgroup observations are independent and identically distributed, are required.

In this paper, we propose the parametric bootstrap control chart for inverse Gaussian percentiles, since neither an explicit formula nor the sampling distribution of a statistic for the inverse Gaussian percentile under a small sample size is available to the best of our knowledge.

This paper is organized as follows. We provide a brief introduction to the inverse Gaussian distribution and maximum likelihood estimation (MLE) of its parameters in Section 2. The procedure of a parametric bootstrap control chart for inverse Gaussian percentiles is presented in Section 3. Through extensive Monte Carlo simulations, the behaviour and performance of the proposed bootstrap control chart is examined in Section 4. This paper ends with discussions and concluding remarks in Section 5.

2. The inverse Gaussian distribution

In this section, we give a brief introduction to the two-parameter inverse Gaussian distribution and MLE of the parameters. The probability density function (pdf) is typically given by

$$f(t;\nu,\lambda)=\sqrt{\frac{\lambda}{2\pi t^3}}\exp\left[-\lambda\frac{(t-\nu)^2}{2\nu^2 t}\right],\quad t>0, \tag{1}$$

where $\nu > 0$ is a location parameter and $\lambda > 0$ is a scale parameter. The cumulative distribution function (cdf) is given by

$$F(t;\nu,\lambda)=\Phi\left[\sqrt{\frac{\lambda}{t}}\left(\frac{t}{\nu}-1\right)\right]+\exp\left(\frac{2\lambda}{\nu}\right)\Phi\left[-\sqrt{\frac{\lambda}{t}}\left(1+\frac{t}{\nu}\right)\right], \tag{2}$$

where $\Phi(\cdot)$ is the standard normal cdf. Note that the coefficient of skewness of the inverse Gaussian distribution is $3\sqrt{\nu/\lambda}$.

Let $\mathcal{T}=\{t_1,t_2,\ldots,t_n\}$ be a random sample of size n from the inverse Gaussian distribution with its pdf in Equation (1). Then the MLEs of location ν and scale λ parameters are given by

$$\hat{\nu}=\bar{t}=\frac{1}{n}\sum_{i=1}^{n}t_i \quad\text{and}\quad \hat{\lambda}=\frac{1}{1/n\sum_{i=1}^{n}t_i^{-1}-1/\bar{t}}. \tag{3}$$

The sampling distributions of $\hat{\nu}$ and $\hat{\lambda}$ have been discussed in detail by Chhikara and Folks [4] and have also been used to construct quality control charts detecting the shifts of centrality and variability for the inverse Gaussian distribution by Edgeman [5,6], Hawkins and Olwell [8] and Sim [9].

Let $F^{-1}(p; \nu, \lambda)$ denote the $100p$th percentile which is obtained by solving the following equation for t

$$F(t; \nu, \lambda) = p. \tag{4}$$

Therefore, the MLE of $100p$th percentile, denoted by $F^{-1}(p; \hat{\nu}, \hat{\lambda})$, is also obtained by solving the following for t

$$F(t; \hat{\nu}, \hat{\lambda}) = p. \tag{5}$$

It should be noted that the solution of Equation (5) can be obtained using some standard mathematical routines for solving the root of a nonlinear equation. In this research, the R package developed by Wheeler [13] is used to solve for Equation (5). It should be noted that in the case that $\lambda \gg \nu$, Equation (5) can be approximated by

$$F(t; \nu, \lambda) \approx \Phi\left[\sqrt{\frac{\lambda}{t}}\left(\frac{t}{\nu} - 1\right)\right], \quad t > 0. \tag{6}$$

Using Equation (6), Onar and Padgett [14] propose an approximated $100p$th percentile for the inverse Gaussian distribution, which is given by

$$s(p; \nu, \lambda) = \frac{\nu^2}{4\lambda}\left(z_p + \sqrt{z_p^2 + \frac{4\lambda}{\nu}}\right)^2, \tag{7}$$

where $z_p = \Phi^{-1}(p)$ is the $100p$th percentile of the standard normal distribution. By the invariance property of the MLE, $s(p; \hat{\nu}, \hat{\lambda})$ is the MLE of $s(p; \nu, \lambda)$. If $\lambda \gg \nu$ is not satisfied, the use of the exact $100p$th percentile, $F^{-1}(p; \nu, \lambda)$, is suggested and the MLE of $100p$th percentile of the inverse Gaussian distribution is then given by $F^{-1}(p; \hat{\nu}, \hat{\lambda})$.

Using the delta method, it may be possible to find an asymptotic distribution of $F^{-1}(p; \hat{\nu}, \hat{\lambda})$ with the sample distributions of $\hat{\nu}$ and $\hat{\lambda}$. Let $F_1(t; \nu, \lambda) = (\partial/\partial t)F(t; \nu, \lambda) = f(t; \nu, \lambda)$, $F_2(t; \nu, \lambda) = (\partial/\partial \nu)F(t; \nu, \lambda)$ and $F_3(t; \nu, \lambda) = (\partial/\partial \lambda)F(t; \nu, \lambda)$. Then it can be shown that

$$\begin{aligned} F_2(t; \nu, \lambda) &= \phi\left[\sqrt{\frac{\lambda}{t}}\left(\frac{t}{\nu} - 1\right)\right]\sqrt{\frac{\lambda}{t}}\left(-\frac{t}{\nu^2}\right) - \frac{2\lambda}{\nu^2}\mathrm{e}^{2\lambda/\nu}\Phi\left[-\sqrt{\frac{\lambda}{t}}\left(1 + \frac{t}{\nu}\right)\right] \\ &\quad - \mathrm{e}^{2\lambda/\nu}\phi\left[-\sqrt{\frac{\lambda}{t}}\left(1 + \frac{t}{\nu}\right)\right]\sqrt{\frac{\lambda}{t}}\left(1 - \frac{t}{\nu^2}\right) \end{aligned} \tag{8}$$

and

$$\begin{aligned} F_3(t; \nu, \lambda) &= \frac{1}{2\sqrt{\lambda}}\phi\left[\sqrt{\frac{\lambda}{t}}\left(\frac{t}{\nu} - 1\right)\right]\left(\frac{\sqrt{t}}{\nu} - \frac{1}{\sqrt{t}}\right) + \frac{2}{\nu}\mathrm{e}^{2\lambda/\nu}\Phi\left[-\sqrt{\frac{\lambda}{t}}\left(1 + \frac{t}{\nu}\right)\right] \\ &\quad - \frac{1}{2\sqrt{\lambda}}\mathrm{e}^{2\lambda/\nu}\phi\left[-\sqrt{\frac{\lambda}{t}}\left(1 + \frac{t}{\nu}\right)\right]\left(\frac{\sqrt{t}}{\nu} + \frac{1}{\sqrt{t}}\right). \end{aligned} \tag{9}$$

Moreover, we have

$$\begin{aligned} \frac{\partial}{\partial \nu}F(F^{-1}(p; \nu, \lambda); \nu, \lambda)) &= F_1(F^{-1}(p; \nu, \lambda); \nu, \lambda)\frac{\partial}{\partial \nu}F^{-1}(p; \nu, \lambda) \\ &\quad + F_2(F^{-1}(p; \nu, \lambda); \nu, \lambda), \end{aligned} \tag{10}$$

$$\begin{aligned} \frac{\partial}{\partial \lambda}F(F^{-1}(p; \nu, \lambda); \nu, \lambda)) &= F_1(F^{-1}(p; \nu, \lambda); \nu, \lambda)\frac{\partial}{\partial \lambda}F^{-1}(p; \nu, \lambda) \\ &\quad + F_3(F^{-1}(p; \nu, \lambda); \nu, \lambda). \end{aligned} \tag{11}$$

Since $F(F^{-1}(p;\nu,\lambda);\nu,\lambda) = p$, Equations (10) and (11) must be zero. It is immediate from Equations (10) and (11) that

$$\frac{\partial}{\partial\nu}F^{-1}(p;\nu,\lambda) = \frac{-F_2(F^{-1}(p;\nu,\lambda);\nu,\lambda)}{f(F^{-1}(p;\nu,\lambda);\nu,\lambda)}, \tag{12}$$

$$\frac{\partial}{\partial\lambda}F^{-1}(p;\nu,\lambda) = \frac{-F_3(F^{-1}(p;\nu,\lambda);\nu,\lambda)}{f(F^{-1}(p;\nu,\lambda);\nu,\lambda)}. \tag{13}$$

Using the first-order Taylor series expansion, we have

$$\begin{aligned} F^{-1}(p;\hat{\nu},\hat{\lambda}) - F^{-1}(p;\nu,\lambda) \approx &- \frac{F_2(F^{-1}(p;\hat{\nu},\hat{\lambda});\hat{\nu},\hat{\lambda})}{f(F^{-1}(p;\hat{\nu},\hat{\lambda});\hat{\nu},\hat{\lambda})}(\hat{\nu}-\nu) \\ &- \frac{F_3(F^{-1}(p;\hat{\nu},\hat{\lambda});\hat{\nu},\hat{\lambda})}{f(F^{-1}(p;\hat{\nu},\hat{\lambda});\hat{\nu},\hat{\lambda})}(\hat{\lambda}-\lambda). \end{aligned} \tag{14}$$

Note that $\hat{\nu}$ has an inverse Gaussian distribution with parameters ν and λn, $n/\hat{\lambda}$ has the $(1/\lambda)\chi^2_{n-1}$ distribution and $\hat{\nu}$ and $n/\hat{\lambda}$ are independent. However, it is quite difficult to find an asymptotic distribution unless either one of the parameters ν and λ is known. In practice, we need to estimate both parameters. In addition, the delta method requires a large sample size to attain a decent accuracy. Thus, we do not consider the Shewhart-type control charts for the inverse Gaussian percentiles using the delta method. This motivates the idea of developing a new parametric bootstrap control chart for the inverse Gaussian percentiles.

3. Construction of a bootstrap control chart

Many authors have studied the application of bootstrap methods to statistical quality control charts. The nonparametric bootstrap method can be applied to control charts, thereby eliminating the traditional parametric assumption. Bootstrap methods can also be applied when the distribution of the statistic used to monitor the process is not available.

Bajgier [15] developed a bootstrap control chart for the process mean, which is a competitor to Shewhart's $\bar{X}$ chart. The only assumption used by Bajgier [15] is that the process is stable and in control when the control limits are computed. If this assumption is not satisfied, when the control limits are computed, the limits become too wide, regardless of the distribution of the process variable. Many papers had indicated that for skewed distributions, bootstrap techniques seemed to have better estimates of the true percentile values on average than the Shewhart-type methods. For a good overview of the bootstrap control chart literature, the reader is referred to [16–18].

Nichols and Padgett [19] developed a parametric bootstrap control chart for the Weibull percentile to monitor the process of producing carbon fibres and compared with the Shewhart-type control charts for percentiles of the Weibull distribution. In terms of the average run lengths (ARL) during the process out-of control, they found the proposed parametric bootstrap method could detect process out-of-control earlier than the Shewhart-type method proposed by Padgett and Spurrier [20].

Since the sampling distribution of statistic for the inverse Gaussian percentile is not available, we propose a parametric bootstrap control chart for the inverse Gaussian percentiles.

The following steps are used for the construction of the bootstrap control chart for the inverse Gaussian percentiles by using the MLEs of ν and λ.

(1) From in-control and stable process, observe k random samples of each size n_j $(j = 1, 2, \ldots, k)$ independently assuming they come from an inverse Gaussian distribution with

unknown location ν and scale λ. We denote the observations of the jth sample by x_{ij} $(i = 1, \ldots, n_j)$. A modified Kolmogorov–Smirnov test proposed by Edgeman *et al.* [21] specifically for the inverse Gaussian distribution should be used to check this assumption. Graphical methods such as Q–Q and P–P plots developed by Onar and Padgett [14] also provide attractive information on checking this assumption. It should be noted that Onar and Padgett [14] used the approximate cdf of the inverse Gaussian distribution to obtain a closed-form quantile function for the Q–Q plot when $\lambda \gg \mu$. In the case where $\lambda \gg \mu$ is not satisfied, we recommend the use of exact quantiles. The R package developed by Wheeler [13] provides the exact quantile of the inverse Gaussian distribution.

(2) Using the MLEs given in Equation (3), evaluate the MLEs of ν and λ with the pooled sample of size $N = \sum_{j=1}^{k} n_j$.

(3) Generate a parametric bootstrap sample of size m, $x_1^*, x_2^* \ldots, x_m^*$, from the inverse Gaussian distribution using the MLEs obtained in Step 2 as the inverse Gaussian distribution parameters. Here, m is the sample size that will be used for future subgroup samples.

(4) Find the MLEs using the bootstrap sample obtained in Step 3 and denote these as $\hat{\nu}^*$ and $\hat{\lambda}^*$.

(5) For the bootstrap subgroup sample obtained in Step 3 and $\hat{\nu}^*$ and $\hat{\lambda}^*$ in Step 4, find the bootstrap estimate, $\hat{W}_p^* = F^{-1}(p; \hat{\nu}^*, \hat{\lambda}^*)$, of the $100p$th percentile $\hat{W}_p = F^{-1}(p; \hat{\nu}, \hat{\lambda})$. In the simulation study, in order to find the inverse Gaussian quantile function $F^{-1}(\cdot)$, we used the R package developed by Wheeler [13].

(6) Repeat Steps 3–5 a large number of times, B, obtaining B bootstrap estimates of $\hat{W}_p$, denoted by $\hat{W}_{p1}^*, \ldots, \hat{W}_{pB}^*$.

(7) Using the B bootstrap estimates obtained in Step 6, find the $100(\gamma/2)$th and $100(1-\gamma/2)$th percentiles. Here, γ is the probability that an observation is considered as out-of-control when the process is actually in control, i.e., false alarm rate (FAR). These $100(\gamma/2)$th and $100(1-\gamma/2)$th percentiles are the LCL and UCL for the bootstrap control chart of FAR=γ, respectively. It should be noted that several versions of the sample percentiles have been suggested in the statistics literature. In the simulation study, we used the method proposed by Hyndman and Fan [22].

Once the control limits have been computed, future subgroup samples of size m are taken from the process at regular time intervals and $F^{-1}(p; \nu, \lambda)$ is estimated for each of the new subgroups by the MLEs, as indicated in Section 2. If the estimate, $\hat{W}_p = F^{-1}(p; \hat{\nu}, \hat{\lambda})$, falls between LCL and UCL calculated in Step 7, the process is assumed to be in control. The values of $\hat{W}_p = F^{-1}(p; \hat{\nu}, \hat{\lambda})$ that are below the LCL or above the UCL signal that the process may be out of control. Hence, once the bootstrap control limits are found, the process is monitored using the statistic $\hat{W}_p = F^{-1}(p; \hat{\nu}, \hat{\lambda})$ in the usual way.

It should be mentioned that the procedures of the bootstrap quality control charts in this section are based on the following principles:

(i) Use all in-control subgroup samples of size n to find MLE estimates of the common unknown population parameters ν and λ. Therefore, the centre line, $\hat{W}_p$, of the bootstrap control charts for the percentiles can be calculated by plugging in the MLEs of ν and λ.

(ii) Use the empirical distribution of B bootstrap samples as the approximated sampling distribution of the monitoring statistic, $\hat{W}_p$ under small sample size m (which could be the same as n) to create the LCL and UCL for the bootstrap control charts of the population percentiles.

(iii) The process is monitored by the corresponding statistic, $\hat{W}_p$, calculated by using each further subgroup sample of small size m generated from the process.

The process is consistent with the process for the Shewhart control charts as well as the process for quality control charts mentioned in the papers. Therefore, the proposed bootstrap control charts are for monitoring for the subgroups of sample size m.

4. Simulation study

The inverse Gaussian distribution provides a suitable model fitting for highly skewed data. However, as Bameni Moghadam and Eskandari [23] pointed out, in many engineering cases, the skewness cannot be easily removed by a transformation. In this section, through the extensive Monte Carlo simulations, we show that the proposed boostrap control charts perform well even for the highly skewed data, R language [24]. For the inverse Gaussian distribution, the R package developed by Wheeler [13] was used. The R program used for this paper can be obtained from the authors upon request.

The behaviour of the bootstrap control charts for the inverse Gaussian distribution is investigated by calculating the average UCL and LCL and their associated standard errors from simulations. The simulations also examine the ARLs and the associated variance for each of the ARLs when the processes are in control and out of control as. The simulations are carried out with different sample sizes, different percentiles of interest and different levels of FARs for many processes. For brevity, we only show some parts of results for the 10th percentile ($p = 0.1$) in Tables 1–12.

The average UCL and LCL and the associated standard errors were computed in the following way: for each set of k independent samples of size $n_j = 5$ ($k = 20$ samples of the same size were used from the simulations) obtained from an inverse Gaussian distribution with a given location parameter, ν, and a given scale parameter, λ, as described in Step 1 of Section 3, Steps 2–7 of Section 3 were then carried out with different bootstrap sample sizes ($m = 5$ or $m = 10$) for B (=10,000) times. This entire process (Steps 1–7) was repeated 10,000 times and the average LCL and the average UCL were computed from 10,000 replications for each different bootstrap sample size, respectively. The standard errors of the control limits were also computed from 10,000 replications for each different bootstrap sample size, respectively. Some of the results are given in Tables 2–3 for bootstrap sample size 5 and in Tables 5–6 for bootstrap sample size 10. As one would expect, when the bootstrap sample size m increased, the control limits get closer together, and in each case of bootstrap sample size, as the percentile is increased from 1% ($p = 0.01$) to 10% ($p = 0.1$) to 50% ($p = 0.5$), the limits become farther apart generally.

Table 1. In-control ARL estimate and its corresponding SD for $p = 0.1$ percentile and $\gamma_0 = 0.1, 0.01, 0.0027, 0.002$ FARs ($n_j = 5$ for $j = 1, \ldots, 20$ and $m = 5$).

	$\lambda = 0.5$		$\lambda = 1.0$		$\lambda = 2.0$	
Parameters	ARL	SD	ARL	SD	ARL	SD
$\gamma_0 = 0.1$ (FAR), $1/\gamma_0 = 10$						
$\nu = 0.5$	9.2323	0.09174735	9.3576	0.09286471	9.4176	0.0918267
$\nu = 1.0$	9.4078	0.09340965	9.2323	0.09174735	9.3245	0.09231789
$\nu = 2.0$	9.2075	0.08965684	9.4078	0.09340965	9.2323	0.09174735
$\gamma_0 = 0.01$ (FAR), $1/\gamma_0 = 100$						
$\nu = 0.5$	92.0059	1.09347536	93.6464	1.14118068	94.1853	1.1995494
$\nu = 1.0$	90.4622	1.05356414	92.0059	1.09347536	93.7985	1.17770798
$\nu = 2.0$	87.7637	1.00045000	90.4622	1.05356414	92.0059	1.09347536
$\gamma_0 = 0.0027$ (FAR), $1/\gamma_0 = 370.37$						
$\nu = 0.5$	356.0655	5.03362987	360.9058	5.08075814	362.6657	5.2130397
$\nu = 1.0$	341.1947	4.53963508	356.0655	5.03362987	356.0550	5.01819249
$\nu = 2.0$	332.4154	4.29985900	341.1947	4.53963508	356.0655	5.03362987
$\gamma_0 = 0.002$ (FAR), $1/\gamma_0 = 500$						
$\nu = 0.5$	478.7813	6.88258104	488.9846	7.13310056	502.0195	7.7748379
$\nu = 1.0$	464.0217	6.82399310	478.7813	6.88258104	490.2206	7.47878357
$\nu = 2.0$	449.1919	5.90723262	464.0217	6.82399310	478.7813	6.88258104

Table 2. In-control LCL and UCL estimates for $p = 0.1$ percentiles and $\gamma_0 = 0.1, 0.01, 0.0027, 0.002$ FARs ($n_j = 5$ for $j = 1, \dots, 20$ and $m = 5$).

	$\lambda = 0.5$		$\lambda = 1.0$		$\lambda = 2.0$	
Parameters	LCL	UCL	LCL	UCL	LCL	UCL
$\gamma_0 = 0.1$ (FAR)						
$\nu = 0.5$	0.070692078	0.307001550	0.115715622	0.373281370	0.172748650	0.421440840
$\nu = 1.0$	0.080061802	0.456635830	0.141384196	0.614001680	0.231316750	0.746679160
$\nu = 2.0$	0.085922140	0.607000780	0.160123670	0.913271160	0.282768670	1.228004930
$\gamma_0 = 0.01$ (FAR)						
$\nu = 0.5$	0.049976633	0.483035690	0.085728192	0.522759870	0.135298833	0.538327040
$\nu = 1.0$	0.054757426	0.819460090	0.099953074	0.966068720	0.171370250	1.046183820
$\nu = 2.0$	0.057579774	1.243502780	0.109514308	1.638923600	0.199906620	1.932144300
$\gamma_0 = 0.0027$ (FAR)						
$\nu = 0.5$	0.043140175	0.593453940	0.075263809	0.608236930	0.121385554	0.600711130
$\nu = 1.0$	0.046726500	1.075441910	0.086280381	1.186908540	0.150451634	1.217150170
$\nu = 2.0$	0.048797814	1.753867700	0.093453271	2.150887100	0.172560570	2.373816400
$\gamma_0 = 0.002$ (FAR)						
$\nu = 0.5$	0.041838506	0.619982230	0.073228824	0.628153570	0.118639525	0.614771030
$\nu = 1.0$	0.045212996	1.140467130	0.083677235	1.239962770	0.146404728	1.256686190
$\nu = 2.0$	0.047172174	1.890907700	0.090426013	2.280934600	0.167354690	2.479932300

Table 3. The standard deviations of the control limits in Table 2.

	$\lambda = 0.5$		$\lambda = 1.0$		$\lambda = 2.0$	
Parameters	LCL	UCL	LCL	UCL	LCL	UCL
$\gamma_0 = 0.1$ (FAR)						
$\nu = 0.5$	0.0000804419	0.0002529143	0.0001114296	0.0002370021	0.0001323337	0.0002016857
$\nu = 1.0$	0.0001014504	0.0004636337	0.0001608868	0.0005058282	0.0002206000	0.0004757272
$\nu = 2.0$	0.0001163454	0.0007196215	0.0002028995	0.0009272563	0.0003217680	0.0010116232
$\gamma_0 = 0.01$ (FAR)						
$\nu = 0.5$	0.0000610989	0.0004320346	0.0000914746	0.0003561038	0.0001185394	0.0002746882
$\nu = 1.0$	0.0000723538	0.0009117096	0.0001221964	0.0008640403	0.0001807314	0.0007173999
$\nu = 2.0$	0.0000801130	0.0016373149	0.0001447030	0.0018234296	0.0002443960	0.0017280794
$\gamma_0 = 0.0027$ (FAR)						
$\nu = 0.5$	0.0000548355	0.0005994294	0.0000843801	0.0004582384	0.0001132867	0.0003394694
$\nu = 1.0$	0.0000635027	0.0013634105	0.0001096717	0.0011988706	0.0001669682	0.0009267517
$\nu = 2.0$	0.0000694562	0.0026730389	0.0001270064	0.0027268928	0.0002193453	0.0023977115
$\gamma_0 = 0.002$ (FAR)						
$\nu = 0.5$	0.0000537281	0.0006475540	0.0000829893	0.0004874311	0.0001124779	0.0003575371
$\nu = 1.0$	0.0000619706	0.0015125387	0.0001074580	0.0012951098	0.0001647080	0.0009877192
$\nu = 2.0$	0.0000675794	0.0030199686	0.0001239415	0.0030251102	0.0002149166	0.0025902021

The in-control ARL was obtained as follows: for each set of $k = 20$ samples of the same size ($n_j = 5$), the control limits were established by Steps 3–7 of Section 3 for each given bootstrap sample size ($m = 5$ or $m = 10$), respectively. Once the control limits were computed, the further subgroup samples of the same bootstrap sample size were continuously generated from the same process and the W_p were estimated by the MLE from the each of further subgroups. The number of times needed for the first estimate, $\hat{W}_p$, out of control limits was recorded as run length. This entire process of obtaining the run length was replicated 10,000 times, and the average of the resulting 10,000 ARLs and the corresponding standard error were calculated.

Table 4. In-control ARL estimate and its corresponding SD for $p = 0.1$ percentile and $\gamma_0 = 0.1, 0.01, 0.0027, 0.002$ FARs ($n_j = 5$ for $j = 1, \ldots, 20$ and $m = 10$).

	$\lambda = 0.5$		$\lambda = 1.0$		$\lambda = 2.0$	
Parameters	ARL	SD	ARL	SD	ARL	SD
$\gamma_0 = 0.1$ (FAR) $1/\gamma_0 = 10$						
$\nu = 0.5$	8.9602	0.08872107	8.8731	0.08817878	8.9362	0.09114803
$\nu = 1.0$	8.8906	0.08781603	8.9602	0.08872107	8.8731	0.08817878
$\nu = 2.0$	8.7195	0.08539058	8.8906	0.08781603	8.9602	0.08872107
$\gamma_0 = 0.01$ (FAR) $1/\gamma_0 = 100$						
$\nu = 0.5$	83.4239	0.99339213	85.7055	1.07298422	84.4841	1.03351367
$\nu = 1.0$	80.3755	0.93978114	83.4239	0.99339213	85.7055	1.07298422
$\nu = 2.0$	79.2814	0.91156766	80.3755	0.93978114	83.4239	0.99339213
$\gamma_0 = 0.0027$ (FAR) $1/\gamma_0 = 370.37$						
$\nu = 0.5$	298.5389	3.92329010	317.1235	4.52902233	321.6831	5.02038653
$\nu = 1.0$	293.1633	3.77553979	298.5389	3.92329010	317.1235	4.52902233
$\nu = 2.0$	290.7581	3.64616863	293.1633	3.77553979	298.5389	3.92329010
$\gamma_0 = 0.002$ (FAR) $1/\gamma_0 = 500$						
$\nu = 0.5$	413.6640	5.90445844	433.3371	6.52552125	441.1853	7.36007219
$\nu = 1.0$	394.3288	5.25322184	413.6640	5.90445844	433.3371	6.52552125
$\nu = 2.0$	393.4395	5.12600840	394.3288	5.25322184	413.6640	5.90445844

Table 5. In-control LCL and UCL estimates for $p = 0.1$ percentiles and $\gamma_0 = 0.1, 0.01, 0.0027, 0.002$ FARs ($n_j = 5$ for $j = 1, \ldots, 20$ and $m = 10$).

	$\lambda = 0.5$		$\lambda = 1.0$		$\lambda = 2.0$	
Parameters	LCL	UCL	LCL	UCL	LCL	UCL
$\gamma_0 = 0.1$ (FAR)						
$\nu = 0.5$	0.0794565560	0.2229821900	0.1279124400	0.2929416700	0.1867929300	0.3522471300
$\nu = 1.0$	0.0911820730	0.3060556600	0.1589125500	0.4459649800	0.2558246700	0.5858823600
$\nu = 2.0$	0.0984059320	0.3780030900	0.1823641200	0.6121110400	0.3178265900	0.8919290400
$\gamma_0 = 0.01$ (FAR)						
$\nu = 0.5$	0.0615503660	0.3068390400	0.1029004640	0.3733039500	0.1568167700	0.4210594800
$\nu = 1.0$	0.0686986830	0.4563963200	0.1231006360	0.6136784700	0.2058010500	0.7466078500
$\nu = 2.0$	0.0728346340	0.6057856000	0.1373971380	0.9127941700	0.2462016200	1.2273569900
$\gamma_0 = 0.0027$ (FAR)						
$\nu = 0.5$	0.0551016580	0.3557939500	0.0934794750	0.4170827800	0.1449611400	0.4564540700
$\nu = 1.0$	0.0608602290	0.5513184300	0.1102033220	0.7115878600	0.1869586700	0.8341661700
$\nu = 2.0$	0.0641093950	0.7613260200	0.1217202440	1.1026350000	0.2204068500	1.4231777000
$\gamma_0 = 0.002$ (FAR)						
$\nu = 0.5$	0.0538233810	0.3673327200	0.0916104740	0.4271018000	0.1425589530	0.4643627800
$\nu = 1.0$	0.0593402890	0.5745131300	0.1076462370	0.7346658600	0.1832213000	0.8542036800
$\nu = 2.0$	0.0624255770	0.8003901400	0.1186803220	1.1490236100	0.2152936600	1.4693333000

Some of the results for the ARLs are listed in Table 1 (for further subgroup sample size $m = 5$) and Table 4 (for further subgroup sample size $m = 10$). Based on a standard theory, we expect the reciprocal of the FAR to be the theoretical ARL. For example, when the FAR is 0.0027, we expect the ARL to be equal to 370. The smaller ARLs indicate that the control limits computed may typically be too narrow, and the ARLs larger than 370 indicate that the control limits computed may be too wide or that the bootstrap control charts give fewer false signals. In general, the empirical ARLs were slightly below the target levels. And when the further subgroup sample size increases, the simulated ARLs decrease.

Table 6. The standard deviations of the control limits in Table 5.

	$\lambda = 0.5$		$\lambda = 1.0$		$\lambda = 2.0$	
Parameters	LCL	UCL	LCL	UCL	LCL	UCL
$\gamma_0 = 0.1$ (FAR)						
$\nu = 0.5$	0.0000876133	0.0001907411	0.0001200557	0.0001958250	0.0001384868	0.0001784863
$\nu = 1.0$	0.0001139553	0.0003209885	0.0001752312	0.0003814832	0.0002401115	0.0003916495
$\nu = 2.0$	0.0001320812	0.0004515703	0.0002279061	0.0006419608	0.0003504625	0.0007629587
$\gamma_0 = 0.01$ (FAR)						
$\nu = 0.5$	0.0000718462	0.0002561370	0.0001048749	0.0002413496	0.0001286134	0.0002058227
$\nu = 1.0$	0.0000892021	0.0004731928	0.0001436930	0.0005122832	0.0002097531	0.0004826938
$\nu = 2.0$	0.0000999588	0.0007210918	0.0001784007	0.0009463870	0.0002873886	0.0010245779
$\gamma_0 = 0.0027$ (FAR)						
$\nu = 0.5$	0.0000664063	0.0003107723	0.0000992038	0.0002791505	0.0001250118	0.0002307631
$\nu = 1.0$	0.0000805833	0.0005964252	0.0001328118	0.0006215513	0.0001984059	0.0005582934
$\nu = 2.0$	0.0000895280	0.0009521557	0.0001611710	0.0011928071	0.0002656207	0.0012431433
$\gamma_0 = 0.002$ (FAR)						
$\nu = 0.5$	0.0000653598	0.0003267618	0.0000980904	0.0002910112	0.0001244742	0.0002383210
$\nu = 1.0$	0.0000790705	0.0006323725	0.0001307148	0.0006535343	0.0001961882	0.0005820351
$\nu = 2.0$	0.0000876733	0.0010211211	0.0001581442	0.0012647491	0.0002614409	0.0013070638

Table 7. Out-of-control ARL estimate and its corresponding SD for $p = 0.1$ percentile and $\gamma_0 = 0.1, 0.01, 0.0027, 0.002$ FARs ($n_j = 5$ for $j = 1, \ldots, 20$ and $m = 5$).

Parameters	FAR	ARL	SD	ARL	SD
		$\lambda_0 = 1.0, \lambda_1 = 0.9$		$\lambda_0 = 1.0, \lambda_1 = 1.1$	
$\nu_0 = 1$	$\gamma_0 = 0.1$	8.1641	0.07998148	10.1099	0.09882115
$\nu_1 = 1$	$\gamma_0 = 0.01$	66.6510	0.84746588	109.9041	1.27521844
	$\gamma_0 = 0.0027$	234.5610	3.32117112	461.9866	6.37238024
	$\gamma_0 = 0.0020$	314.6847	4.80034290	639.6701	9.36906247
		$\nu_0 = 1.0, \nu_1 = 0.9$		$\nu_0 = 1.0, \nu_1 = 1.1$	
$\lambda_0 = 1$	$\gamma_0 = 0.1$	10.0604	0.1008229	8.6136	0.08621968
$\lambda_1 = 1$	$\gamma_0 = 0.01$	111.4855	1.4093647	74.6570	0.82924842
	$\gamma_0 = 0.0027$	448.7198	6.7172956	266.2708	3.38639463
	$\gamma_0 = 0.0020$	636.2406	9.9944078	358.1544	4.75293900

Table 8. Out-of-control LCL and UCL estimates of Table 7 for $p = 0.1$ percentiles and $\gamma_0 = 0.1, 0.01, 0.0027, 0.002$ FARs ($n_j = 5$ for $j = 1, \ldots, 20$ and $m = 5$).

Parameters	FAR	LCL	UCL	LCL	UCL
		$\lambda_0 = 1.0, \lambda_1 = 0.9$		$\lambda_0 = 1.0, \lambda_1 = 1.1$	
$\nu_0 = 1$	$\gamma_0 = 0.1$	0.1416274590	0.6137941700	0.1415105710	0.6135740300
$\nu_1 = 1$	$\gamma_0 = 0.01$	0.1001706160	0.9647506900	0.1000655310	0.9643561900
	$\gamma_0 = 0.0027$	0.0864853960	1.1850007600	0.0863594960	1.1846359900
	$\gamma_0 = 0.0020$	0.0838779710	1.2381006200	0.0837607020	1.2379716900
		$\nu_0 = 1.0, \nu_1 = 0.9$		$\nu_0 = 1.0, \nu_1 = 1.1$	
$\lambda_0 = 1$	$\gamma_0 = 0.1$	0.1416560600	0.6141188400	0.1412936060	0.6132078500
$\lambda_1 = 1$	$\gamma_0 = 0.01$	0.1001630820	0.9654162000	0.0999024890	0.9645120000
	$\gamma_0 = 0.0027$	0.0864675760	1.1859558200	0.0862462860	1.1848005400
	$\gamma_0 = 0.0020$	0.0838729980	1.2392224800	0.0836312240	1.2381154100

Next, we evaluate the performance of bootstrap control chart monitoring the out-of-control processes. First, the control limits of the in-control process were established and then these were used to monitor the estimated percentiles $\hat{W}_p$ calculated from the further subgroup sample generated from the out-of-control process of different parameters. In this paper, we particularly

Table 9. Out-of-control LCL and UCL estimates of Table 7 for $p = 0.1$ percentiles and $\gamma_0 = 0.1, 0.01, 0.0027, 0.002$ FARs ($n_j = 5$ for $j = 1, \ldots, 20$ and $m = 5$).

Parameters	FAR	LCL	UCL	LCL	UCL
		$\nu_0 = 1.0, \nu_1 = 0.5$		$\nu_1 = 1.5, \lambda_1 = 1.5$	
$\nu_0 = 1$	$\gamma_0 = 0.1$	0.0001623895	0.0005094371	0.0001575754	0.0004983925
$\nu_1 = 1$	$\gamma_0 = 0.01$	0.0001233103	0.0008645099	0.0001196690	0.0008565789
	$\gamma_0 = 0.0027$	0.0001106571	0.0011885010	0.0001075175	0.0011876643
	$\gamma_0 = 0.0020$	0.0001085927	0.0012828859	0.0001051465	0.0012859803
		$\nu_0 = 1.0, \nu_1 = 0.9$		$\nu_0 = 1.0, \nu_1 = 1.1$	
$\lambda_0 = 1$	$\gamma_0 = 0.1$	0.0001614992	0.0005122311	0.0001617500	0.0005073019
$\lambda_1 = 1$	$\gamma_0 = 0.01$	0.0001221989	0.0008747749	0.0001229543	0.0008669840
	$\gamma_0 = 0.0027$	0.0001096035	0.0012080178	0.0001101169	0.0011943946
	$\gamma_0 = 0.0020$	0.0001074455	0.0013045858	0.0001078214	0.0012975191

Table 10. Out-of-control ARL estimates and its corresponding SD for $p = 0.1$ percentile and $\gamma_0 = 0.1, 0.01, 0.0027, 0.002$ FARs ($n_j = 5$ for $j = 1, \ldots, 20$ and $m = 5$).

Parameters	FAR	ARL	SD	ARL	SD
		$\nu_1 = 0.5, \lambda_1 = 0.5$		$\nu_1 = 1.5, \lambda_1 = 1.5$	
$\nu_0 = 1$	$\gamma_0 = 0.1$	2.0367	0.01542	4.6637	0.0444369
$\lambda_0 = 1$	$\gamma_0 = 0.01$	5.1155	0.056314	26.1076	0.3018681
	$\gamma_0 = 0.0027$	9.2255	0.117720	75.6938	0.9858286
	$\gamma_0 = 0.0020$	10.6520	0.148011	96.9108	1.3361881
		$\nu_1 = 0.9, \lambda_1 = 1.1$		$\nu_1 = 1.1, \lambda_1 = 0.9$	
$\nu_0 = 1$	$\gamma_0 = 0.1$	11.5069	0.1150229	7.7312	0.07520027
$\lambda_0 = 1$	$\gamma_0 = 0.01$	150.1939	1.7786145	59.1829	0.69061493
	$\gamma_0 = 0.0027$	694.9974	10.2466568	197.4657	2.66379078
	$\gamma_0 = 0.0020$	997.3532	15.0137909	259.5024	3.59759399

Table 11. Out-of-control LCL and UCL estimates of Table 10 for $p = 0.1$ percentiles and $\gamma_0 = 0.1, 0.01, 0.0027, 0.002$ FARs ($n_j = 5$ for $j = 1, \ldots, 20$ and $m = 5$).

Parameters	FAR	LCL	UCL	LCL	UCL
		$\lambda_1 = 0.5, \lambda_1 = 0.5$		$\lambda_1 = 1.5, \lambda_1 = 1.5$	
$\nu_0 = 1$	$\gamma_0 = 0.1$	0.1415445180	0.6138580300	0.1415069600	0.6131758000
$\lambda_0 = 1$	$\gamma_0 = 0.01$	0.1000859970	0.9649412000	0.1000695130	0.9635580300
	$\gamma_0 = 0.0027$	0.0863982950	1.1856329900	0.0864046890	1.1840658000
	$\gamma_0 = 0.0020$	0.0838039400	1.2385103100	0.0837890480	1.2373658900
		$\nu_1 = 0.9, \lambda_1 = 1.1$		$\nu_1 = 1.1, \lambda_1 = 0.9$	
$\nu_0 = 1$	$\gamma_0 = 0.1$	0.1413500700	0.6135553000	0.1415822430	0.6131532800
$\lambda_1 = 1$	$\gamma_0 = 0.01$	0.0999387600	0.9650301000	0.1001306740	0.9635116100
	$\gamma_0 = 0.0027$	0.0862495390	1.1852444000	0.0864576660	1.1832896000
	$\gamma_0 = 0.0020$	0.0836418760	1.2384460500	0.0838348660	1.2363893000

Table 12. The standard deviations of the control limits in Table 11.

Parameters	FAR	LCL	UCL	LCL	UCL
		$\nu_1 = 0.5, \lambda_1 = 0.5$		$\nu_1 = 1.5, \lambda_1 = 1.5$	
$\nu_0 = 1$	$\gamma_0 = 0.1$	0.0001613453	0.0005129893	0.0001613806	0.0005081992
$\lambda_0 = 1$	$\gamma_0 = 0.01$	0.0001223480	0.0008733275	0.0001223752	0.0008687047
	$\gamma_0 = 0.0027$	0.0001096476	0.0012061065	0.0001097618	0.0012028782
	$\gamma_0 = 0.0020$	0.0001071839	0.0013040020	0.0001074232	0.0013005135
		$\nu_1 = 0.9, \lambda_1 = 1.1$		$\nu_1 = 1.1, \lambda_1 = 0.9$	
$\nu_0 = 1$	$\gamma_0 = 0.1$	0.0001595826	0.0005048414	0.0001608862	0.0005099032
$\lambda_0 = 1$	$\gamma_0 = 0.01$	0.0001211291	0.0008664106	0.0001223485	0.0008680475
	$\gamma_0 = 0.0027$	0.0001084015	0.0011960082	0.0001097683	0.0012002113
	$\gamma_0 = 0.0020$	0.0001059927	0.0012929996	0.0001074738	0.0012993147

examine the process shift from in-control process with $\nu_0 = 1.0$ and $\lambda_0 = 1.0$ to out-of-control process with either one parameter different from 1.0 or with both parameters different from 1.0. For brevity, we only show part of simulation results in Tables 7–12. Tables 8 and 11 show LCLs and UCLs for monitoring the cases of out-of-control processes, and the corresponding out-of-control ARLs are given in Tables 7 and 10, respectively. Tables 9 and 12 show the corresponding standard errors of LCLs and UCLs which are reported in Tables 8 and 11, respectively. The simulation differences among LCLs and UCLs and among the corresponding standard errors are negligible, since the LCLs and UCLs and the corresponding standard errors were simulated under the control processes with $\nu_0 = 1.0$ and $\lambda_0 = 1.0$ for all the cases.

In summary, for the case of the out-of-control process with the shift of λ_0 to λ_1, the control chart is more sensitive to signal the out-of-control for the case where λ_1 is slightly below 1.0 than for the case where λ_1 is slightly above 1.0. When the out-of-control process is due to the shift of ν_0 to a ν_1, the control chart is more sensitive to signal the out-of-control when ν_1 is slightly above 1.0 than when ν_1 is slightly below 1.0. For the case of the out-of-control process with the shifts of two parameters, the control chart is more sensitive to signal out-of-control when λ_1 slightly decreases from 1.0 and ν_1 slightly increases from 1.0 than when λ_1 slightly increases from 1.0 and ν_1 slightly decreases from 1.0. Moreover, the control chart is sensitive to signal the out-of-control when both ν and λ moderately increase or more from 1.0 and also when both ν and λ moderately decrease or more from 1.0.

5. Discussion and concluding remarks

It should be mentioned again that the $100p$th percentile, $s(p; \nu, \lambda)$ in Equation (7), which is proposed by Onar and Padgett [14], is an approximate percentile and works well enough only when $\lambda \gg \nu$. In the case where $\lambda \gg \nu$ is not satisfied, the use of the exact $100p$th percentile, $F^{-1}(p; \nu, \lambda)$, is suggested. The approximate percentile function $s(p; \nu, \lambda)$ is increasing in ν and decreasing in λ when $p > 0.5$. But, if $p < 0.5$, $s(p; \nu, \lambda)$ is increasing in both ν and λ. The exact inverse Gaussian quantile function, $F^{-1}(p; \nu, \lambda)$, has the same tendency when p is not near 0.5. Using this idea, Onar and Padgett [14] provide the Bonferroni confidence bounds which can be used for constructing control charts.

To compare the performance of the proposed bootstrap control charts with the control charts based on the Bonferroni confidence bounds, we carried out numerical simulations. The approximate percentile function $s(p; \hat{\nu}, \hat{\lambda})$ in Equation (7) was used in Table 13 and the exact quantile function, $F^{-1}(p; \hat{\nu}, \hat{\lambda})$, was used in Table 14. Note that Tables 13 and 14 correspond to Table 1 of the proposed bootstrap control charts in Section 4. Comparing Table 1 with Tables 13 and 14, we can see that the results clearly show that the proposed bootstrap control charts outperform. The empirical ARLs shown in Tables 13 and 14 are far away from their respective target values than those shown in Table 1 using the bootstrap method.

Currently, there is no existing closed-form solution relating the inverse Gaussian percentile to its underlying parameters (ν and λ). In addition, the sampling distribution of the statistic for the inverse Gaussian percentile is not available. Thus, the conventional Shewhart-type control chart for the inverse Gaussian percentile is not tractable. Moreover, the control charts based on Bonferroni's concept with $s(p; \hat{\nu}, \hat{\lambda})$ or $F^{-1}(p; \hat{\nu}, \hat{\lambda})$ used clearly underperform the proposed bootstrap control charts in terms of the ARL. Therefore, we proposed the use of a bootstrap control chart in order to deal with the issues described.

The proposed bootstrap control chart seems to be reasonably effective and can be easily implemented for the case where one needs to assume the inverse Gaussian distribution for the probability of process measurements. However, the results show that the resulting in-control ARLs indicate that the empirical FARs are generally larger than the target FARs. This implies that the quality

Table 13. In-control ARL estimate and its corresponding SD for $p = 0.1$ percentile and $\gamma_0 = 0.1, 0.01, 0.0027, 0.002$ FARs ($n_j = 5$ for $j = 1, \ldots, 20$ and $m = 5$), using the Bonferroni bounds and $F^{-1}(p; \nu, \lambda)$.

	$\lambda = 0.5$		$\lambda = 1.0$		$\lambda = 2.0$	
Parameters	ARL	SD	ARL	SD	ARL	SD
$\gamma_0 = 0.1$ (FAR), $1/\gamma_0 = 10$						
$\nu = 0.5$	6.5662	0.06758534	8.4541	0.08936883	10.3444	0.1089418
$\nu = 1.0$	5.4791	0.05431272	6.5662	0.06758534	8.4541	0.08936883
$\nu = 2.0$	4.7516	0.04549963	5.4791	0.05431272	6.5662	0.06758534
$\gamma_0 = 0.01$ (FAR), $1/\gamma_0 = 100$						
$\nu = 0.5$	35.6995	0.41786835	65.4889	0.84222716	105.7277	1.3306956
$\nu = 1.0$	21.0491	0.24058516	35.6995	0.41786835	65.4889	0.84222716
$\nu = 2.0$	13.7576	0.15076358	21.0491	0.24058516	35.6995	0.41786835
$\gamma_0 = 0.0027$ (FAR), $1/\gamma_0 = 370.37$						
$\nu = 0.5$	86.4608	1.03689930	200.2168	2.71792890	379.5907	5.0817415
$\nu = 1.0$	40.3959	0.47112951	86.4608	1.03689930	200.2168	2.71792890
$\nu = 2.0$	23.0827	0.26041952	40.3959	0.47112951	86.4608	1.03689930
$\gamma_0 = 0.002$ (FAR), $1/\gamma_0 = 500$						
$\nu = 0.5$	105.6785	1.29830512	256.1609	3.40067939	503.7040	6.7598239
$\nu = 1.0$	46.4601	0.54021559	105.6785	1.29830512	256.1609	3.40067939
$\nu = 2.0$	25.8932	0.29307929	46.4601	0.54021559	105.6785	1.29830512

Table 14. In-control ARL estimate and its corresponding SD for $p = 0.1$ percentile and $\gamma_0 = 0.1, 0.01, 0.0027, 0.002$ FARs ($n_j = 5$ for $j = 1, \ldots, 20$ and $m = 5$), Using the Bonferroni bounds and $s(p; \nu, \lambda)$.

	$\lambda = 0.5$		$\lambda = 1.0$		$\lambda = 2.0$	
Parameters	ARL	SD	ARL	SD	ARL	SD
$\gamma_0 = 0.1$ (FAR), $1/\gamma_0 = 10$						
$\nu = 0.5$	15.2467	0.1613203	16.3860	0.1853784	16.8553	0.1876983
$\nu = 1.0$	13.4277	0.1449599	15.2467	0.1613203	16.3860	0.1853784
$\nu = 2.0$	11.7715	0.1255631	13.4277	0.1449599	15.2467	0.1613203
$\gamma_0 = 0.01$ (FAR), $1/\gamma_0 = 100$						
$\nu = 0.5$	110.5408	1.3511718	159.5936	2.0676980	199.3510	2.6222842
$\nu = 1.0$	70.2553	0.8331852	110.5408	1.3511718	159.5936	2.0676980
$\nu = 2.0$	46.0691	0.5216213	70.2553	0.8331852	110.5408	1.3511718
$\gamma_0 = 0.0027$ (FAR), $1/\gamma_0 = 370.37$						
$\nu = 0.5$	311.4768	4.1009280	540.8017	7.5948381	767.9347	11.3556765
$\nu = 1.0$	155.1935	2.0131246	311.4768	4.1009280	540.8017	7.5948381
$\nu = 2.0$	85.8753	0.9776572	155.1935	2.0131246	311.4768	4.1009280
$\gamma_0 = 0.002$ (FAR), $1/\gamma_0 = 500$						
$\nu = 0.5$	385.7149	5.0374979	702.5761	9.8879447	1044.5276	15.1195500
$\nu = 1.0$	184.9644	2.3724879	385.7149	5.0374979	702.5761	9.8879447
$\nu = 2.0$	97.9095	1.1379746	184.9644	2.3724879	385.7149	5.0374979

engineer who wants to use the inverse Gaussian model needs to take caution in deciding on the value of the target FARs he wants. In future research, we hope to develop a more accurate parametric bootstrap control chart that will resolve this overshooting FAR problem.

Acknowledgements

The authors wish to thank Professor W.J. Padgett of Statistics at the University of South Carolina and of Mathematical Sciences at Clemson University for his encouragement throughout this research. The authors also would like to thank associate editor and anonymous referees for their comments and suggestions which significantly improved this manuscript.

References

[1] G.K. Bhattacharyya and A. Fries, *Fatigue failure models-Birnbaum-Saunders vs. inverse Gaussian*, IEEE Trans. Reliab. 31 (1980), pp. 439–440.
[2] F. Desmond, *Stochastic models of failure in random environments*, Can. Stat. 13 (1985), pp. 171–183.
[3] C.J. Goh, L.C. Tang, and S.C. Lim, *Reliability modelling of stochastic wear-out failure*, Reliab. Eng. Sys. Safety 25 (1989), pp. 303–314.
[4] R.S. Chhikara and J.L. Folks, *The Inverse Gaussian Distribution*, Marcel Dekker, Inc., New York and Basel, 1990.
[5] R.L. Edgeman, *Inverse Gaussian control charts*, Aust. J. Stat. 31 (1989), pp. 78–84.
[6] R.L. Edgeman, *Control of inverse Gaussian processes*, Qual. Eng. 1 (1989), pp. 265–276.
[7] R.L. Edgeman, *SPRT & CUSUM results for inverse Gaussian processes*, Commun. Stat. Theory Methods 25 (1996), pp. 2797–2806.
[8] D.M. Hawkins and D.H. Olwell, *Inverse Gaussian cumulative sum control charts for location and shape*, Statistician 46 (1997), pp. 323–335.
[9] C.H. Sim, *Inverse Gaussian control charts for Monitoring Process Variability*, Commun. Stat. Simul. Comput. 32 (2003), pp. 223–239.
[10] B. Efron and R.J. Tibshirani, *An Introduction to the Bootstrap*, Chapman and Hall, New York, 1993.
[11] B. Gunter, *Bootstrapping: how to make something from almost nothing and get statistically valid answers, Part III*, Qual. Progr. 25 (1992), pp. 119–122.
[12] G.A. Young, *Bootstrap: more than a stab in the dark*, Stat. Sci. 9 (1994), pp. 382–415.
[13] B. Wheeler, *SuppDists: Supplementary distributions*, R package version 1.1-2, 2008, http://cran.r-project.org/web/packages/SuppDists/
[14] A. Onar and W.J. Padgett, *Accelerated test models with the inverse Gaussian distribution*, J. Stat. Plann. Infer. 89 (2000), pp. 119–133.
[15] S.M. Bajgier, *The use of bootstrapping to construct limits on control charts*, Proceedings of the Decision Science Institute, San Diego, CA, 1992, pp. 1611–1613.
[16] T. Seppala, H. Moskowitz, R. Plante, and J. Tang, *Statistical process control via the subgroup bootstrap*, J. Qual. Technol, 27 (1995), pp. 139–153.
[17] R.Y. Liu and J. Tang, *Control charts for dependent and independent measurements based on the bootstrap*, J. Amer. Stat. Assoc. 91 (1996), pp. 1694–1700.
[18] L.A. Jones and W.Y. Woodall, *The performance of bootstrap control charts*, J. Qual. Techn. 30 (1998), pp. 362–375.
[19] M.D. Nichols and W.J. Padgett, *A bootstrap control chart for Weibull percentiles*, Qual. Reliab. Eng. Int. 22 (2005), pp. 141–151.
[20] W.J. Padgett and J.D. Spurrier, *Shewhart-type charts for percentiles of strength distributions*, J. Qual. Technol. 22 (1990), pp. 283–288.
[21] R.L. Edgeman, R.C. Scott, and R.J. Pavur, *A modified Kolmogorov-Smirnov test for inverse Gaussian distribution with unknown parameters*, Commun. Stat. Ser. B Simul. Comp. 17 (1988), pp. 1203–1212.
[22] R.J. Hyndman and Y. Fan, *Sample quantiles in statistical packages*, Amer. Stat. 50 (1996), pp. 361–365.
[23] M. Bameni Moghadam, and F. Eskandari, *Quality improvement by using inverse Gaussian model in robust engineering*, Qual. Quan. 40 (2006), pp. 157–174.
[24] R Development Core Team, *R: A Language and Environment for Statistical Computing*, R Foundation for Statistical Computing, Vienna, Austria 2006. ISBN: 3-900051-07-0.